JOURNAL OF SOLID STATE CHEMISTRY 76, 40–51 (1988)

Hydrous Phase in the Crystalline Vanadium Oxide Spheres

S. KITTAKA, S. SASAKI, N. OGAWA, AND N. UCHIDA

Department of Chemistry, Faculty of Science, Okayama University of Science, 1-1 Ridaicho, Okayama 700, Japan

Received December 7, 1987; in revised form March 8, 1988

The presence of a hydrous phase was investigated in fine crystalline V_2O_5 spheres which contain a cavity inside. A high-resolution electron micrograph shows the formation of hydrous V_2O_5 in the grain boundaries between V_2O_5 crystallites. The experiments using sorption of gases, thermal desorption spectroscopy (TDS), and IR spectroscopy have suggested that the hydrous phase is composed mainly of a layered compound, probably $V_2O_5 \cdot 1.6H_2O$. The physisorption of water was almost completely reversible up to a relative pressure of 0.3. The interlayer spacings seems to work as sorption sites. When H_2O is sorbed as a monolayer, determined by applying the BET equation to the sorption isotherm, the hydrous phase is identified as $V_2O_5 \cdot 2.6H_2O$. Most of the H_2O molecules in the hydrous phase can be removed below 200°C; removal of oxygen commences at 250°C in vacuum. Various states of H_2O phase were demonstrated TDS with peaks at 100, 170, 260, and 420°C. The heating of V_2O_5 spheres in O_2 at 300–400°C produces a mosaic particle with monocrystalline (010) surfaces.

Introduction

Crystalline fine sphere of vanadium oxide (V_2O_5) with interior cavities were recently produced by the present authors by passing V_2O_5, V_2O_3, and NH_4VO_3 powders through an O_2–H_2 flame at 2000°C (*1*). The particles range from 20 to 500 nm in diameter and expose only (010) crystal planes to the exterior; i.e., a particle is a mosaic structure compound in which single crystallites of V_2O_5 radially direct their ⟨010⟩ axis outward from the core cavity of the sphere. Thus, this material is expected to have uniform crystal planes as well as many grain boundaries between the crystallites: each particle therefore should have a high proportion of crystallographically imperfect regions. It has been understood that amorphous V_2O_5 dissolves readily in water to form hydrous V_2O_5, gel, or sol, depending upon the ratio of H_2O to the solid, but that crystalline V_2O_5 is insoluble in H_2O (*2*). The V_2O_5 spheres were, as a matter of fact, formed by thermal decomposition and oxidation reactions of the raw materials in high temperature water vapor, i.e., under hydrothermal condition. Thus, it is interesting to know the effect of high temperature H_2O on the physicochemical properties of characteristic parts of the crystalline V_2O_5 spheres described above.

The aim of the present work is to examine the homogeneity of the V_2O_5 sphere surface and its affinity for and stability toward H_2O molecules. The techniques used are gas adsorption, thermal desorption spectroscopy (TDS), infrared spectroscopy

0022-4595/88 $3.00

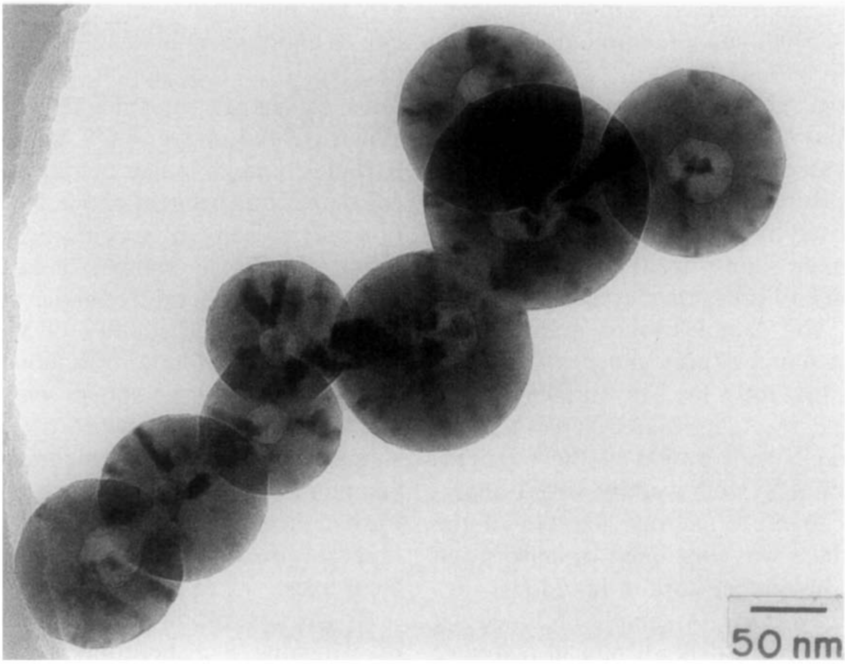

FIG. 1. Electron micrograph of V_2O_5 spheres formed by O_2–H_2 flame fusion at 2000°C.

(IR), X-ray diffraction (XRD), and high-resolution electron microscopy (HREM).

Experimental

Materials. The preparation of vanadium oxide spheres was detailed in a previous paper (*1*). The sample studied here is from a portion collected on the G-2 gauze where the fine V_2O_5 spheres could most efficiently be obtained. Figure 1 shows an electron micrograph of some sample spheres in which the single crystal domains have grown from the surface to the core cavity. Lattice fringes and X-ray diffraction analyses substantiated that these particles crystallized as orthorhombic V_2O_5. A superstructure of V_2O_5 was found in some locations of the particle, suggesting the presence of oxygen defects; in other words, vanadium ions having valencies less than 5. Some comparative investigations were made on crystalline V_2O_5 which was prepared by pyrolysis of NH_4VO_3, in air at 400°C for 5 hr, as raw material for V_2O_5 spheres.

Thermal desorption spectroscopy. The amount of gas that evolved from V_2O_5 spheres by heating was determined by barometric and gravimetric methods (*3, 4*). In the former technique, a portion of desorbed gas was led from the main vacuum line to a Baratron capacitance manometer set up with a 1-Torr (133 Pa) pressure sensor unit. In the latter, the weight loss of the sample was determined by use of a Cahn 2000 electrobalance. Before each measurement the sample was evacuated at 25°C overnight. The background pressure of the system before increasing the temperature was below 10^{-3} Pa and a liquid N_2 trap was used, ahead of the vacuum pump, to avoid the contamination of the sample with oil. The heating rate, 1.67°C min^{-1}, was controlled by Programmed Temperature Controller EC5100, manufactured by Ohkura Elec. Co.

Sorption. The H_2O vapor sorption was carried out gravimetrically on a 300-mg sample with the electrobalance used in the TDS measurement. The vapor pressure was adjusted by regulating the temperature of the water supply from −55 to 25°C so that the rate of pressure increase was ca. 50 Pa hr^{-1}. The samples were preheated at increasing temperatures under vacuum and in an O_2 flow for 4 hr. The surface area of the sample was determined separately by volumetric N_2 adsorption at the temperature of liquid N_2, followed by a BET analysis. The degree of atomic flatness of the solid surface was examined by adsorption of Kr at the temperature of liquid N_2.

IR spectroscopy. A sample of 30–40 mg was pressed to a disk 20 mm in diameter under a pressure of 1 ton cm^{-2}. The disk was preheated in a silica glass cell having single-crystal NaCl windows. The IR spectrometer used Type IR-G manufactured by Nippon Bunko Co.

Electron microscopy. The effect of heat treatment on the structural change of the sample was studied using a high-resolution electron microscope together with XRD. The preheated samples were suspended in acetone and deposited over the microgrids prepared with triafor over the copper grid (No. 200). The electron microscope was a JEOL-2000EX instrument operated at an accelerating voltage of 200 kV. The samples were observed at direct magnifications below 200,000, above which high-resolution photographs could not be obtained.

Results and Discussion

Change in crystallinity and surface homogeneity of the V_2O_5 spheres. Figures 2a–2h constitute a series of electron micrographs for samples heated in vacuum and in O_2. The heat treatment of the sample gave rise to an increase in degree of crystallinity and led to a straightening of grain boundaries at temperatures higher than 200°C. When treated above 400°C in vacuum the particle could no longer maintain its spherical shape; this brought about the formation of a polyhedron with a central cavity, composed of a small number of larger single crystals. At temperatures higher than 600°C the component crystallites of V_2O_5 in the sphere grew into large orthogonal crystals and the cavity in the sphere was lost (Fig. 2f). When the particle was heated in O_2, its shape changed at lower temperature than in vacuum (Figs. 2a and 2h), and all particles formed orthogonal crystallites at 500°C, the longest direction of growth being along ⟨100⟩ axes.

Kr gas adsorption is a useful method for investigating the smoothness of the solid surface on an atomic scale (*5*). When the solid surface is completely flat and the experiment is carried out below the two-dimensional critical temperature (−168°C), an adsorption isotherm having several steps is obtained (*6, 7*). Figure 3 shows the adsorption isotherms of Kr for V_2O_5 spheres heated in O_2 at increasing temperatures. The V_2O_5 spheres show two steps at low pressures $P/P_0 = 0$ and 0.01, but no truly vertical step is seen. The latter small step suggests the presence of a small proportion of a homogeneous area. By increasing the treatment temperature to 400°C, a steep rise was observed at $P/P_0 = 0.002$ and the step at 0.01 became less pronounced. Thus, we could obtain a V_2O_5 sample with a geometrically uniform (010) plane when the V_2O_5 spheres were heated in O_2 at 300–400°C (Fig. 2g). Adsorption of Kr on the samples evacuated at increasing temperatures did not lead to isotherms, suggesting a homogeneity of the surface.

Desorbable substances from V_2O_5 spheres. Figure 4 shows the TDS of V_2O_5 spheres and of V_2O_5 raw material. Two

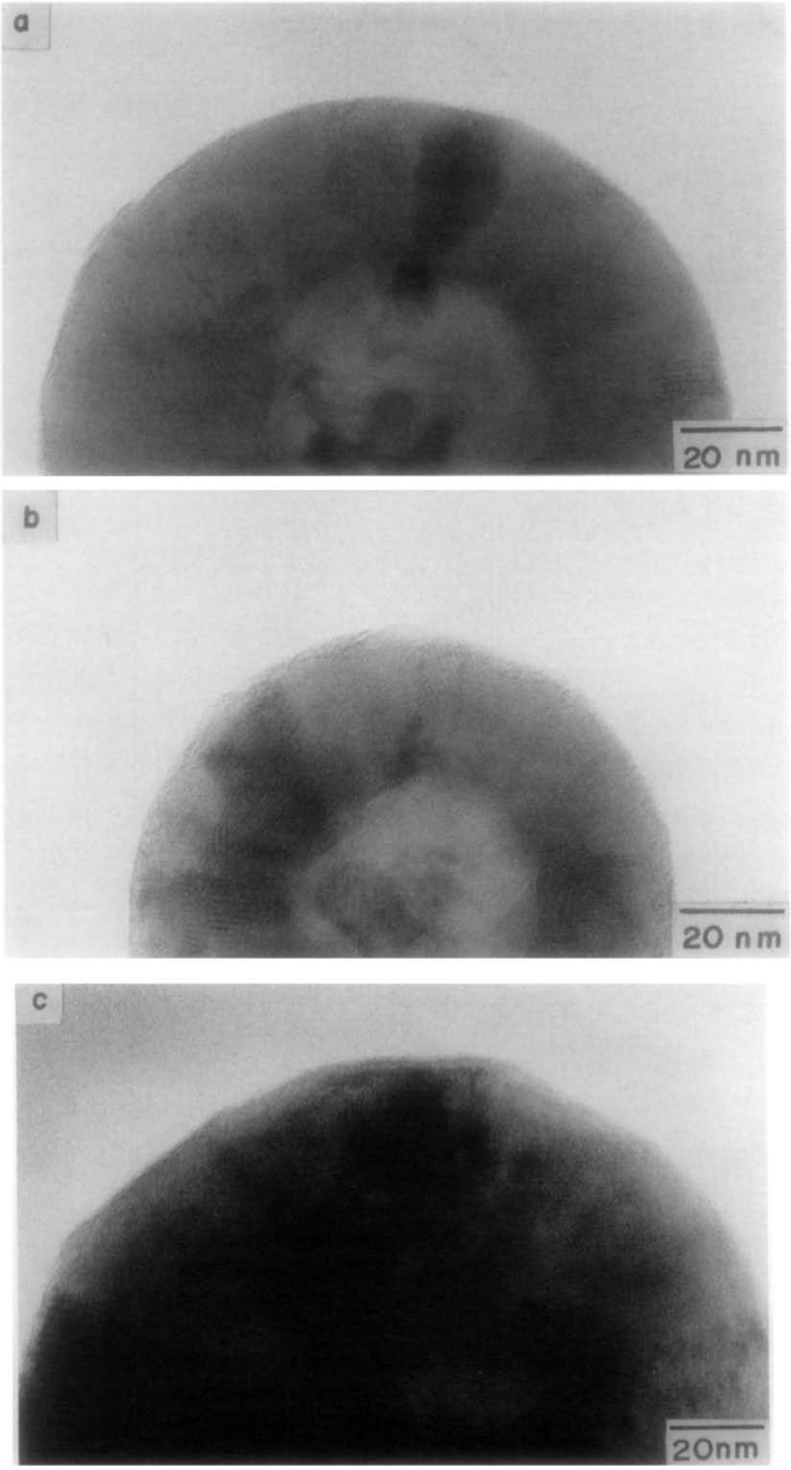

FIG. 2. Electron micrographs of V_2O_5 spheres heated at increasing temperatures. In vacuum: (a) sample sphere; (b) 200°C; (c) 300°C; (d) 400°C; (e) 500°C; (f) 600°C. In O_2: (g) 400°C; (h) 500°C.

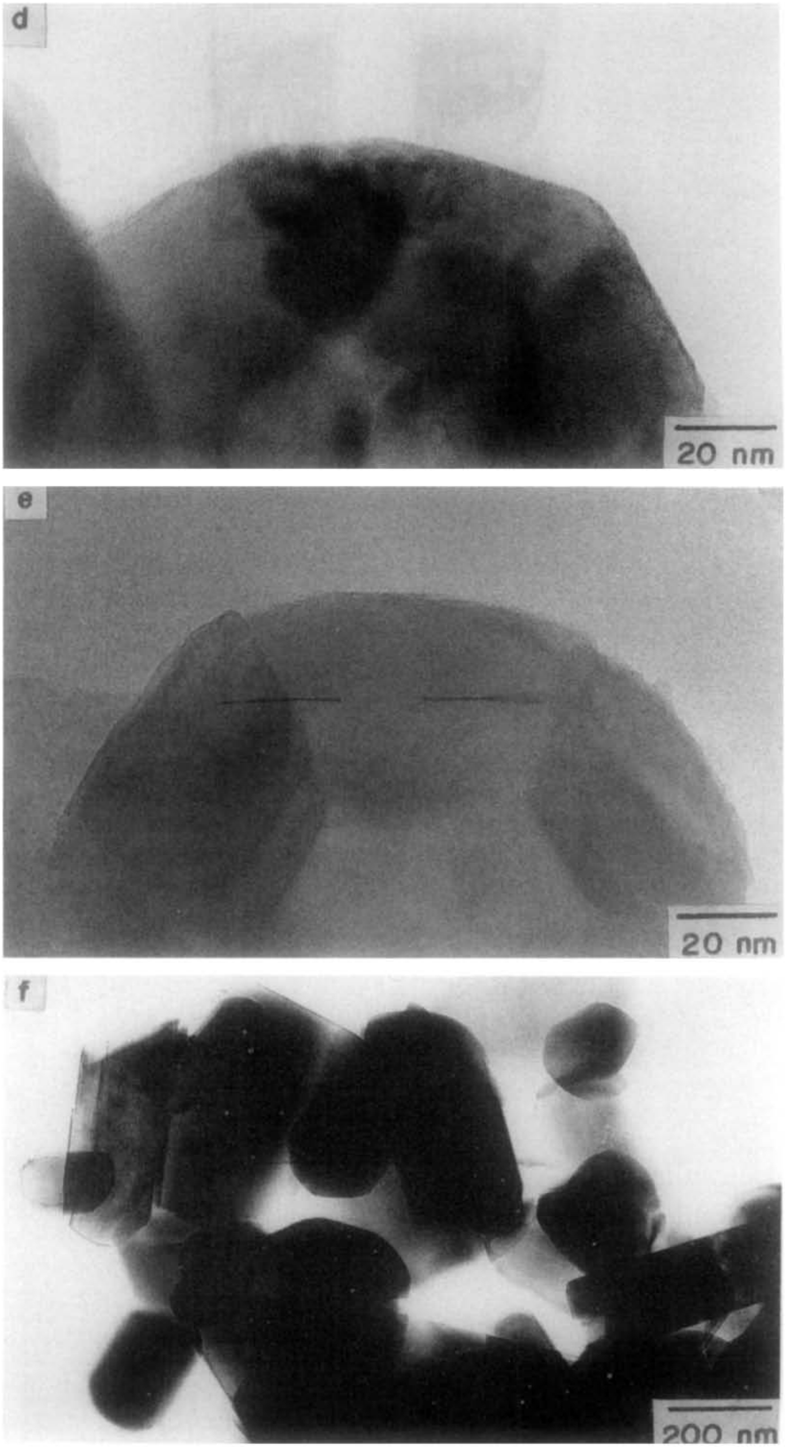

FIG. 2—*Continued.*

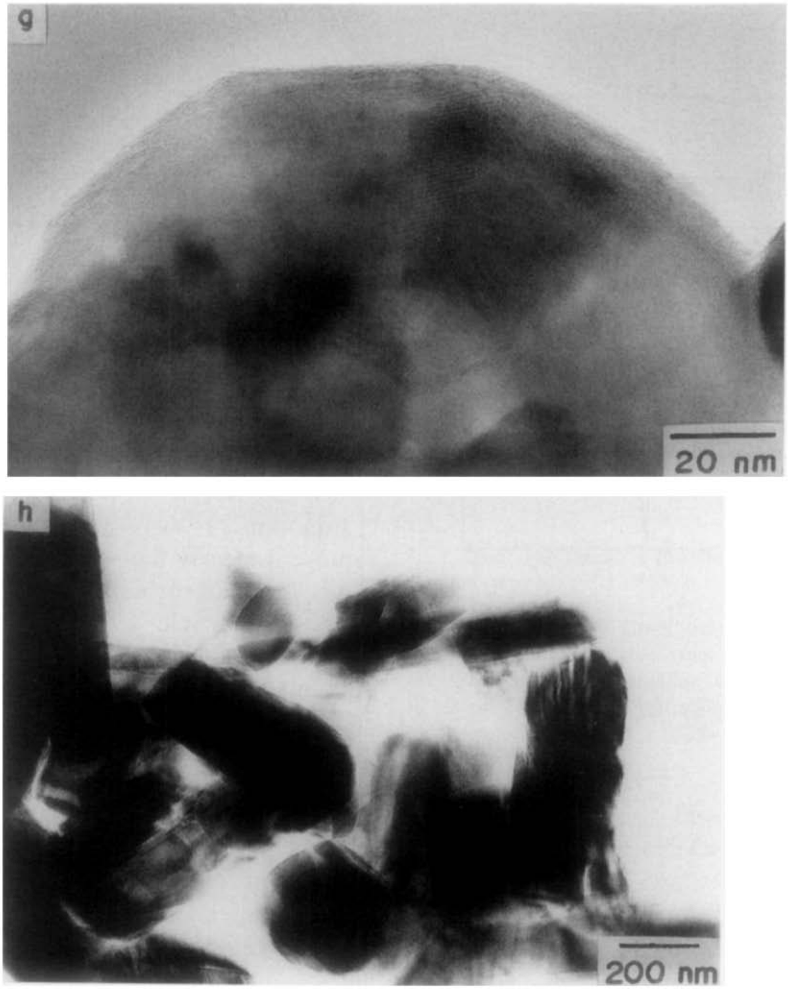

FIG. 2—*Continued.*

large desorption peaks (P-1 close to 90–100°C and P-2 at 310°C in which some small shoulders were included) appeared in both curve 1 (barometric) and curve 2 (gravimetric) of the V_2O_5 spheres. On the other hand, a much smaller P-1 was obtained for the raw V_2O_5 (curve 4, barometric). The ratio of P-1 to P-2 ($R_g = 1.24$) determined in the gravimetric method (curve 2) is much larger than that observed by the barometric method ($R_b = 0.68$, curve 1) where a deconvolution of the two peaks was somewhat arbitrarily made at the minimum point between the two. This difference between the two observations may be interpreted as follows: the peak obtained by barometric TDS should in principle be proportional to the molar amount of the desorbed substance, while that by the gravimetric method should be proportional to the mass of the desorbed gas: $R_b = n_2/n_1$ and $R_g = n_2M_2/n_1M_1$, where n and M denote the mole number and molecular weight of the desorbed gas, respectively. The ratio $R_g/R_b = M_2/M_1$ provides information on the two species producing the two peaks. This ratio

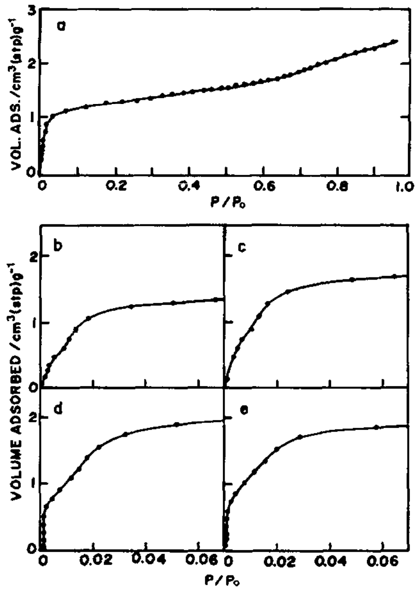

FIG. 3. Adsorption isotherms of Kr on V_2O_5 spheres heated in 1 atm O_2 at increasing temperatures. (a) Full isotherm for the V_2O_5 spheres; (b) enlarged isotherm for a low pressure range; (c) V_2O_5 spheres heated at 200°C; (d) 300°C; (e) 400°C.

is roughly 1.83. Peak 1 was assigned to the desorption of H_2O from the IR measurements described below. If P-2 is assumed to be due to the desorption of oxygen, the ratio $R_g/R_b = M_{O_2}/M_{H_2O} = 1.78$, which is close to the experimental value. The XRD analyses confirmed that evacuation at temperatures higher than 300°C gave rise to the V_2O_4 and other complex phases in the sample. Thus, P-1 and P-2 may be ascribed to the desorption of H_2O and O_2, respectively. The gravimetric TDS of V_2O_5 spheres determined in a flow of O_2 (ca. 50 ml min^{-1}, curve 3) yielded a P-1 of almost the same intensity as that in vacuum, but appearing at somewhat higher temperatures. P-2 has disappeared almost completely, and the small peaks at 260 (P-3) and 410°C (probably shifted P-4) became more marked compared to the small shoulders in P-2 in vacuum. The whole TDS sequence in O_2 is very similar to the results of DTA–TGA for $V_2O_5 \cdot 1.6H_2O$ gels reported by Aldebert *et al.* (*8*) and by Abello and Pommier (*9*). That is, each stage of weight loss (P-1, P-3, and P-4) may be assigned to the endothermic reaction (*2–4*) respectively shown below:

$$V_2O_5 \cdot 3H_2O = V_2O_5 \cdot 1.6H_2O + 1.4H_2O \quad (1)$$

$$V_2O_5 \cdot 1.6H_2O = V_2O_5 \cdot 0.5H_2O + 1.1H_2O \quad (2)$$

$$V_2O_5 \cdot 0.5H_2O = V_2O_5 \cdot 0.1H_2O + 0.4H_2O \quad (3)$$

$$V_2O_5 \cdot 0.1H_2O = V_2O_5 + 0.1H_2O. \quad (4)$$

Equation (1) was additionally used to represent clearly the sequence of the reactions. If the desorbed H_2O (P-1) is spread over the particle evenly (46 molecules nm^{-2}), the number of stacking monolayers amounts to ca. 5. But as can be seen in Fig. 2a, the growth of the component crystal domains extend almost to the surface. Thus, such a large amount of H_2O should be detected in some special phase of the sample particle. Allowing for the great number of crystallographically imperfect regions, especially many grain boundaries, it is suggested that the H_2O molecules desorbed close to 90°C originate in the grain

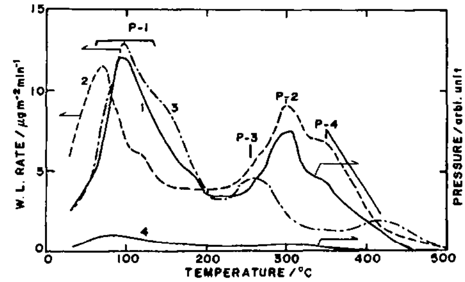

FIG. 4. Thermal desorption spectra (TDS) for V_2O_5 spheres and raw V_2O_5. (1) Barometrically determined TDS(B) for V_2O_5 spheres; (2) gravimetrically determined TDS(G) for V_2O_5 spheres in a vacuum; (3) TDS(G) for V_2O_5 spheres in 1 atm O_2; (4) TDS(B) for raw V_2O_5. Heating rate is 1.67°C min^{-1}.

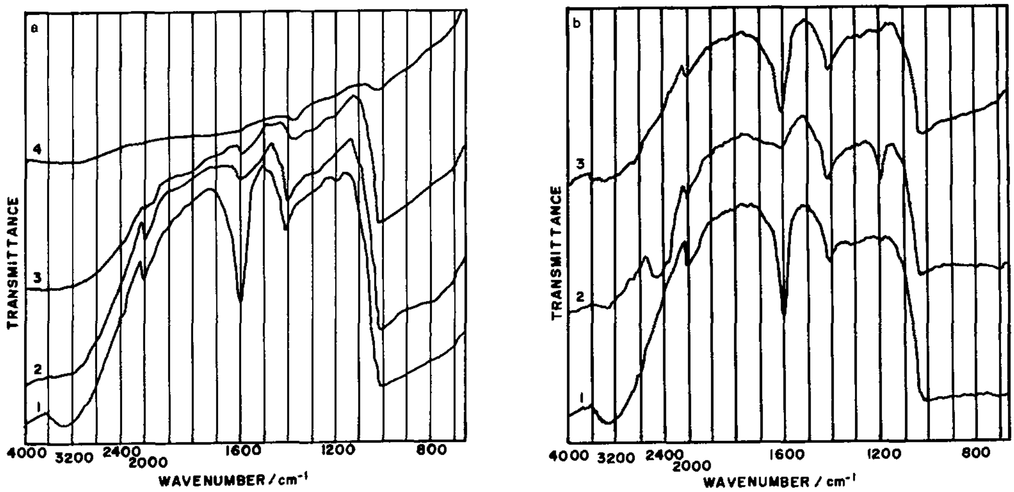

FIG. 5(a) IR spectra for V_2O_5 spheres heated in vacuum at increasing temperatures. (1) Room temperature; (2) 200°C; (3) 300°C; (4) 350°C. (b) Effect of deuteration on the IR spectra of V_2O_5 spheres. (1) Evacuated at room temperature; (2) deuterated after the cycling of exposing D_2O vapor and evacuation five times after process 1; (3) hydrated through the cycling of exposing H_2O vapor and evacuation after process 2.

boundaries between the V_2O_5 crystallites, probably as component water of hydrous V_2O_5 ($V_2O_5 \cdot 1.6H_2O$).

Figure 5a shows the IR spectra of V_2O_5 spheres which have been evacuated at increasing temperatures. The absorption bands at 3350 and 1600 cm^{-1} decrease markedly on heating above 200°C. On contacting with D_2O vapor at room temperature, these two bands were replaced by new bands at 2500 and 1200 cm^{-1} (Fig. 5b). The former two bands (3360 cm^{-1} due to the stretching mode of OH and 1600 cm^{-1} due to the bending mode of OH) reappeared upon treatment with H_2O vapor. Thus, it may be concluded that the substances desorbed by heating below 200°C are strongly sorbed H_2O molecules. Vandenborre *et al.* (*10*) have investigated the orientation of H_2O molecules between layers in $V_2O_5 \cdot 1.6H_2O$ and in $V_2O_5 \cdot 0.5H_2O$ by use of polarized IR spectroscopy, in which the fine structure around 3500 cm^{-1} changes, depending on the angle of the incident light. The appearance of a single peak in the present case can rationally be explained by a random orientation of the hydrous phase. The transparency of IR through the sample decreased markedly on evacuation at temperatures higher than 250°C and was accompanied by darkening of the sample. Thus, it may be claimed that peak 2 in TDS of Fig. 4 is due to the desorption of O_2, i.e., the formation of black Magnéli phases of $V_{2n}O_{5n-1}$.

Sorption of H_2O on the V_2O_5 spheres. Figure 6a shows the first sorption isotherms of H_2O by V_2O_5 spheres just after evacuating at increasing temperatures from room temperature to 500°C. Figure 6b shows the second sorption isotherms of H_2O of samples evacuated at 25°C for 1 night after the initial sorption of H_2O. The first isotherms are lowered toward the abscissa by drastic heating at temperatures higher than 300°C. A similar change was observed in the second sorption isotherms of Fig. 6b, but the shape of the isotherms changed into type 2 from the complicated shapes of the first sorption curves (Fig. 6a). The latter

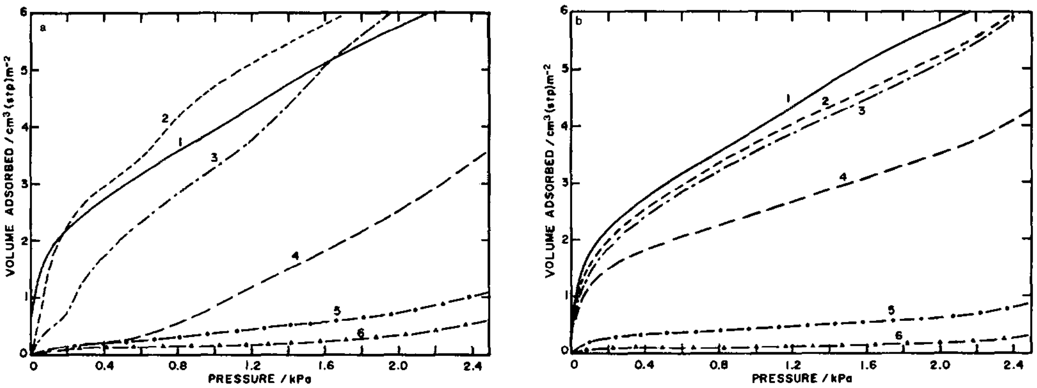

FIG. 6(a) Sorption isotherms (first) of H_2O at 25°C for the V_2O_5 spheres heated in vacuum at increasing temperatures. (1) 25°C; (2) 100°C; (3) 200°C; (4) 300°C; (5) 400°C; (6) 500°C. (b) Sorption isotherms (second) of H_2O at 25°C for V_2O_5 spheres determined after the first adsorption in (a).

result can be explained by the fact that the dehydrated surface is rehydrated during the first sorption of H_2O. The second sorption isotherms for the samples pretreated at less than 200°C are similar to each other. These results signify that samples heated at low temperatures can be rehydrated during the first sorption. This reversibility of interaction of H_2O with solid has been reported by Abello and Pommier (*9*). The apparent monolayer volumes, V_m in Table I which have been determined by use of BET equation for the spheres treated at temperatures below 200°C, are much larger than the theoretical monolayer volume, $V_m^0 = 0.36$ cm³(stp) m^{-2} calculated by assuming the molecular area of H_2O to be 0.106 nm². These large V_m values (roughly six times V_m^0) suggest that sorption of H_2O is not limited only to the surface but also occurs in the interior regions of the particles.

When the sample was heated in O_2 at increasing temperatures, a marked drop of V_m was found at temperatures lower than those in evacuated samples (Table I), but the trend was similar. The monolayer capacity for Kr and N_2 did not change significantly upon heating, which is different from the case for H_2O. Thus again, the decrease of H_2O sorption by heating should not be

TABLE I

THE SURFACE AREA (S) AND APPARENT MONOLAYER VOLUMES (V_m) OF H_2O ON V_2O_0 SPHERES AS DETERMINED BY APPLYING BET EQUATION ON THE SECOND SORPTION ISOTHERMS

	Evacuated		O_2 treated	
Temperature (°C)	S (m² g^{-1})	V_m (cm³(stp) m^{-2})	S (m² g^{-1})	V_m (cm³(stp) m^{-2})
25	8.22	2.31	—	—
100	9.04	2.19	10.05	2.28
200	9.15	2.05	11.2	2.01
300	9.39	1.58	12.2	0.188
400	9.44	0.297	11.6	0.108
500	9.44	0.110	9.37	0.067

TABLE II

THE SURFACE AREA (S) AND MONOLAYER VOLUMES FOR THE FIRST AND SECOND ADSORPTION OF H_2O ON THE RAW V_2O_5 POWDER

Temperature (°C)	S ($m^2 g^{-1}$)	V_{m_1} (cm^3(stp) m^{-2})	V_{m_2} (cm^3(stp) m^{-2})
25	10.2	0.0903	0.0923
100	11.0	0.114	0.0923
200	11.2	0.144	0.131
300	11.3	0.153	0.124
400	11.2	0.135	0.124
500	11.4	0.119	0.103

ascribed just to some change on the surface, but mainly to the decrease in sorption sites in the particles.

The sorption isotherms of H_2O for the raw V_2O_5 samples heated in vacuum at increasing temperatures belong to type 2 (Table II). The V_m values of these are all smaller than the calculated one of V_m^0 which permits us to assign the sorption to adsorption on the surface only. The V_m values for the first adsorption increase with temperature up to 300°C and decrease at higher temperatures. In the second adsorption, the V_m values for samples evacuated at room temperature, 100, and 200°C coincide with each other, implying that the sites for physical adsorption of H_2O, i.e., surface hydroxyls, were reproduced during the first adsorption of H_2O. In other words, surface hydroxyls on the V_2O_5 were reproducibly removed by heating. A gradual decrease in isotherms at higher temperatures has often been observed on metal oxide surfaces (*11*, *12*), although the reason for this has not yet been clarified. The sorption of H_2O on crystalline V_2O_5 occurs only on the solid surface; this confirms the hypothesis that large amounts of H_2O sorption on the V_2O_5 spheres cannot be attributed to the native surface properties of crystalline V_2O_5. Flat surfaces of the samples treated in O_2 at 300 through 400°C did not give rise to a stepwise sorption isotherm for H_2O, contrary to the case of homogeneous surfaces of Cr_2O_3 (*11*) and SnO_2 (*12*, *13*).

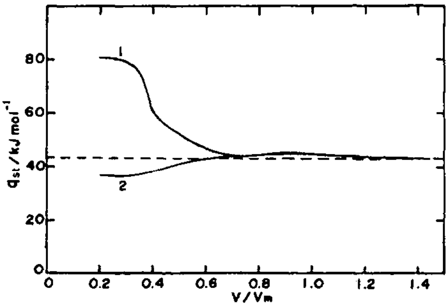

FIG. 7. Isosteric heat of sorption of H_2O for the sample V_2O_5 spheres (1) and raw V_2O_5 (2). Broken line represents the heat of condensation of H_2O.

Hydrous Phase in the V_2O_5 Spheres. In order to obtain information concerning the exceptionally high V_m values for the second sorption on V_2O_5 spheres, isosteric differential heats of sorption (q_{st}) were measured. When the sorption proceeds on the preheated sample up to saturated vapor pressure, the sorption isotherm rises rapidly after each repetition of H_2O sorption, while the raw crystalline V_2O_5 does not display this feature. This result indicates that the spheres have increased their capacity for H_2O molecules in a higher humidity. The sorption of H_2O was then carried out below a relative pressure of 0.3, by changing the temperature of sorption from 10 to 25°C by 5°. Figure 7 shows the q_{st} curves for sample V_2O_5 spheres and raw V_2O_5 powder, the

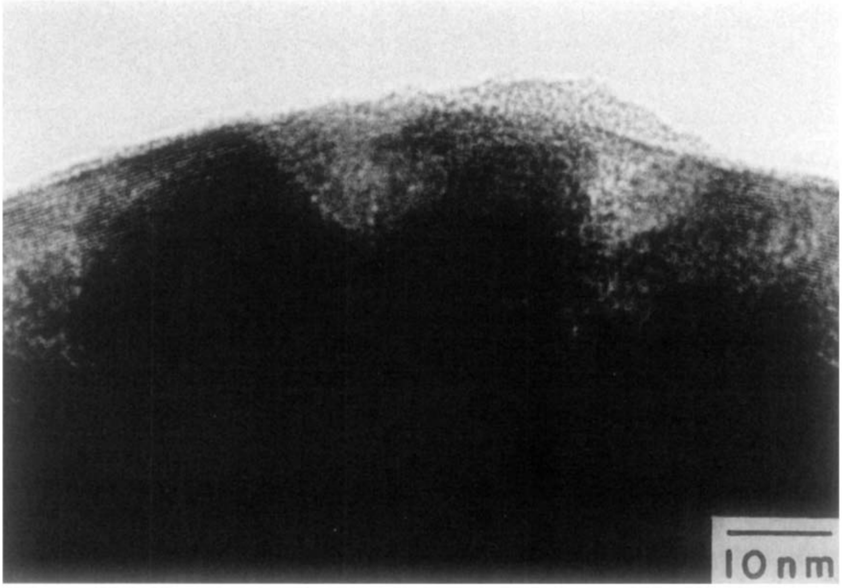

FIG. 8. High-resolution electron micrograph of the V_2O_5 sphere surface after being in contact with saturated H_2O vapor for 4 hr.

latter being a particle of orthogonal shape. Here, q_{st} values were plotted as a function of the adsorbed amount divided by V_m (V/V_m). The q_{st} for raw V_2O_5 is very low at low coverages and increases gradually toward the heat of condensation of H_2O. This means that the V_2O_5 surface is originally hydrophobic, as is the case for silica (*14*) and heated iron oxide (*15*) surfaces. The q_{st} value for V_2O_5 spheres is as high as 75 kJ mole^{-1} below $V/V_m = 0.4$ and converges to ca. 45 kJ mole^{-1} above $V/V_m = 0.4$, which is close to the heat of condensation of H_2O. These q_{st} values seem to be directly related to the heats of hydration of hydrous V_2O_5 described by Eqs. (2) and (1), i.e., 70 and 42 kJ mole^{-1}, determined respectively by Abello and Pommier by DTA (*9*).

The electron microscope studies did not reveal a hydrous phase in the original V_2O_5 spheres (Fig. 1a). However, when the sample was exposed to saturated H_2O vapor for more than 2 hr, damage or channels were clearly observed along the boundaries between component crystallites (Fig. 8). After longer hydration the sample was completely hydrated and formed a layered compound; the details of this process will be reported in a separate paper. Thus it is reasonable to believe that there are small hydrous V_2O_5 phases in the grain boundaries of the V_2O_5 spheres and that they grow in high humidity even at room temperature.

Finally, we should comment upon the situation of the hydrous V_2O_5 phase which is covered by H_2O at V_m. If we assume P-1 of curve 2 in Fig. 4 is due to reaction (2) and that 40% of V_m of H_2O sorption is due to the back reaction (2), the H_2O content per 1 mole V_2O_5, involved in the H_2O sorption, is found to be ca. $2.6H_2O$ at the state where the amount of sorbed H_2O is equal to V_m. This might indicate that some stable phase proceeds to a higher stage of hydration than $V_2O_5 \cdot 1.6H_2O$; Abello and Pommier (*9*) have proposed the establishment of a phase $V_2O_5 \cdot 3H_2O$ through Eq. (1).

References

1. S. Kittaka, S. Sasaki, and T. Morimoto, *J. Mater. Sci.* **22,** 557 (1987).
2. J. Livage, N. Gharbi, M. C. Leroy, and M. Michaud, *Mater. Res. Bull.* **13,** 117 (1978).
3. K. Morishige, F. Kanno, S. Ogawara, and S. Sasaki, *J. Phys. Chem.* **89,** 4404 (1985).
4. K. Morishige, S. Kittaka, T. Moriyasu, and T. Morimoto, *J. Chem. Soc. Faraday Trans.* 1 **76,** 738 (1980).
5. S. Ross and J. P. Olivier, "On Physical Adsorption," p. 123, Wiley, New York (1964).
6. A. Thomy and J. Duval, *J. Chim. Phys.* **66,** 1966 (1969).
7. A. Thomy, X. Duval, and J. Regier, *Surf. Sci. Rep.* **1,** 1 (1981).
8. P. Aldebert, N. Baffier, N. Gharbi, and J. Livage, *Mater. Res. Bull.* **16,** 669 (1981).
9. L. Abello and C. Pommier, *J. Chim. Phys.* **80,** 373 (1983).
10. M. T. Vandenborre, R. Prost, E. Huard, and J. Livage, *Mater. Res. Bull.* **18,** 1133 (1983).
11. S. Kittaka, K. Morishige, J. Nishiyama, and T. Morimoto, *J. Colloid Interface Sci.* **91,** 117 (1983).
12. K. Morishige, S. Kittaka, and T. Morimoto, *J. Colloid Interface Sci.* **89,** 86 (1982).
13. S. Kittaka, K. Morishige, T. Fujimoto, and T. Morimoto, *J. Colloid Interface Sci.* **72,** 191 (1979).
14. A. C. Zettlemoyer, "Hydrophobic Surface" (F. M. Fowks, Ed.), p. 1, Academic Press, New York (1969).
15. T. Morimoto, Y. Yokota, and M. Nagao, *J. Colloid Interface Sci.* **64,** 188 (1978).